PYGS
Research article
Proceedings of the Yorkshire Geological Society
https://doi.org/10.1144/pygs2022-007 | Vol. 64 | 2022 | pygs2022-007

A new subsurface record of the Pliensbachian–Toarcian, Lower Jurassic, of Yorkshire

João P. Trabucho-Alexandre[1,2*], Darren R. Gröcke[1], Elizabeth Atar[1], Liam Herringshaw[3] and Ian Jarvis[4]

[1] Department of Earth Sciences, Durham University, Durham DH1 3LE, UK
[2] Department of Earth Sciences, Universiteit Utrecht, 3584 CB Utrecht, The Netherlands
[3] Hidden Horizons, The Fossil Shop, Scarborough YO11 1NH, UK
[4] Department of Geography, Geology and the Environment, Kingston University London, Kingston upon Thames KT1 2EE, UK

JPT, 0000-0003-1997-027X; DRG, 0000-0003-2296-7530; EA, 0000-0003-1921-022X; LH, 0000-0001-5216-7126; IJ, 0000-0003-3184-3097
* Correspondence: j.trabucho@uu.nl

Abstract: Here, we describe the upper Pliensbachian to middle Toarcian stratigraphy of the Dove's Nest borehole, which was drilled near Whitby, North Yorkshire, in 2013. The core represents a single, continuous vertical section through unweathered, immature Lower Jurassic sedimentary rocks. The thickness of the Lias Group formations in the Dove's Nest core is approximately the same as that exposed along the North Yorkshire coast between Hawsker Bottoms and Whitby. The studied succession consists of epeiric-neritic sediments and comprises cross-laminated very fine sandstones, (oolitic) ironstones, and argillaceous mudstones. Dark argillaceous mudstone is the dominant lithology. These sediments were deposited in the Cleveland Basin, a more subsident area of an epeiric sea, the Laurasian Sea.

We present a set of geochemical data that includes organic carbon isotope ratios ($\delta^{13}C_{org}$) and total organic carbon (TOC). The $\delta^{13}C_{org}$ record contains a negative excursion across the Pliensbachian–Toarcian boundary and another in the lower Toarcian that corresponds to the Toarcian Oceanic Anoxic Event (T-OAE). Below the T-OAE negative excursion, $\delta^{13}C_{org}$ values are less ^{13}C-depleted than above it. We find no evidence of a long-term $\delta^{13}C_{org}$ positive excursion. TOC values below the T-OAE negative excursion are lower than above it.

Sedimentary evidence suggests that, during much of the Pliensbachian–Toarcian interval, the seafloor of the Cleveland Basin was above storm wave-base and that storm-driven bottom currents were responsible for much sediment erosion, transport, and redeposition during the interval of oceanic anoxia. The abrupt shifts observed in the $\delta^{13}C_{org}$ record (lower Toarcian) are likely to reflect the impact of erosion by storms on the morphology of the $\delta^{13}C$ record of the T-OAE.

Supplementary material: stratigraphic and geochemical data [organic carbon isotope ratios ($\delta^{13}C_{org}$) and total organic carbon (TOC)] are available at https://doi.org/10.6084/m9.figshare.c.6154436

Received 14 April 2022; **revised** 5 August 2022; **accepted** 15 August 2022

The Lower Jurassic succession exposed along the North Yorkshire coast, between Redcar and Ravenscar (Fig. 1), is one of the most extensively studied successions of Jurassic marine sediments (Hemingway 1974; Cope *et al.* 1980; Rawson and Wright 1995; Powell 2010). The succession consists of epeiric-neritic sediments and comprises hummocky cross-stratified sandstones, (oolitic) ironstones, and argillaceous mudstones deposited in an epeiric sea, the Laurasian Sea. Dark argillaceous mudstone is the dominant lithology. During the Early Jurassic, even though the seafloor of the epeiric sea was relatively level, differential subsidence resulted in areas in which a thicker and more carbonaceous Lower Jurassic succession accumulated (Hallam and Sellwood 1976; Ziegler 1981, 1990; Howarth 1992; Adrichem Boogaert and Kouwe 1993–1997; Jenkyns and Clayton 1997; Caswell and Coe 2012; Jenkyns and Macfarlane 2022). The Lower Jurassic sediments of North Yorkshire accumulated in a small basin, the Cleveland Basin (Fig. 1), which was an extension of the Sole Pit, Broad Fourteens, and West Netherlands basins.

The lower Toarcian of the Cleveland Basin includes an interval (Semicelatum and Exaratum subzones) that is characterized by dark carbonaceous mudstones, or black shales, that contain a large negative excursion in organic carbon isotope ratios ($\delta^{13}C_{org}$) (Hesselbo *et al.* 2000; Kemp *et al.* 2005). These black shales were deposited during the Toarcian Oceanic Anoxic Event (T-OAE). The increase in the rate of burial of ^{13}C-depleted organic carbon during the early Toarcian is thought to have been due to oceanic anoxia (e.g. French *et al.* 2014; Thibault *et al.* 2018; Houben *et al.* 2021) and physiographic restriction of the Laurasian Sea (e.g. McArthur *et al.* 2008; Baroni *et al.* 2018; Remírez and Algeo 2020).

An excellent stratigraphic framework for the Lower Jurassic of North Yorkshire that is still in use today was established by several authors between 1955 and 1985 (Howarth 1955, 1962, 1973; Cope *et al.* 1980; Powell 1984; Howard 1985). Using this stratigraphic framework, the presence of several distinctive concretionary horizons in the succession makes it straightforward to identify the age of the

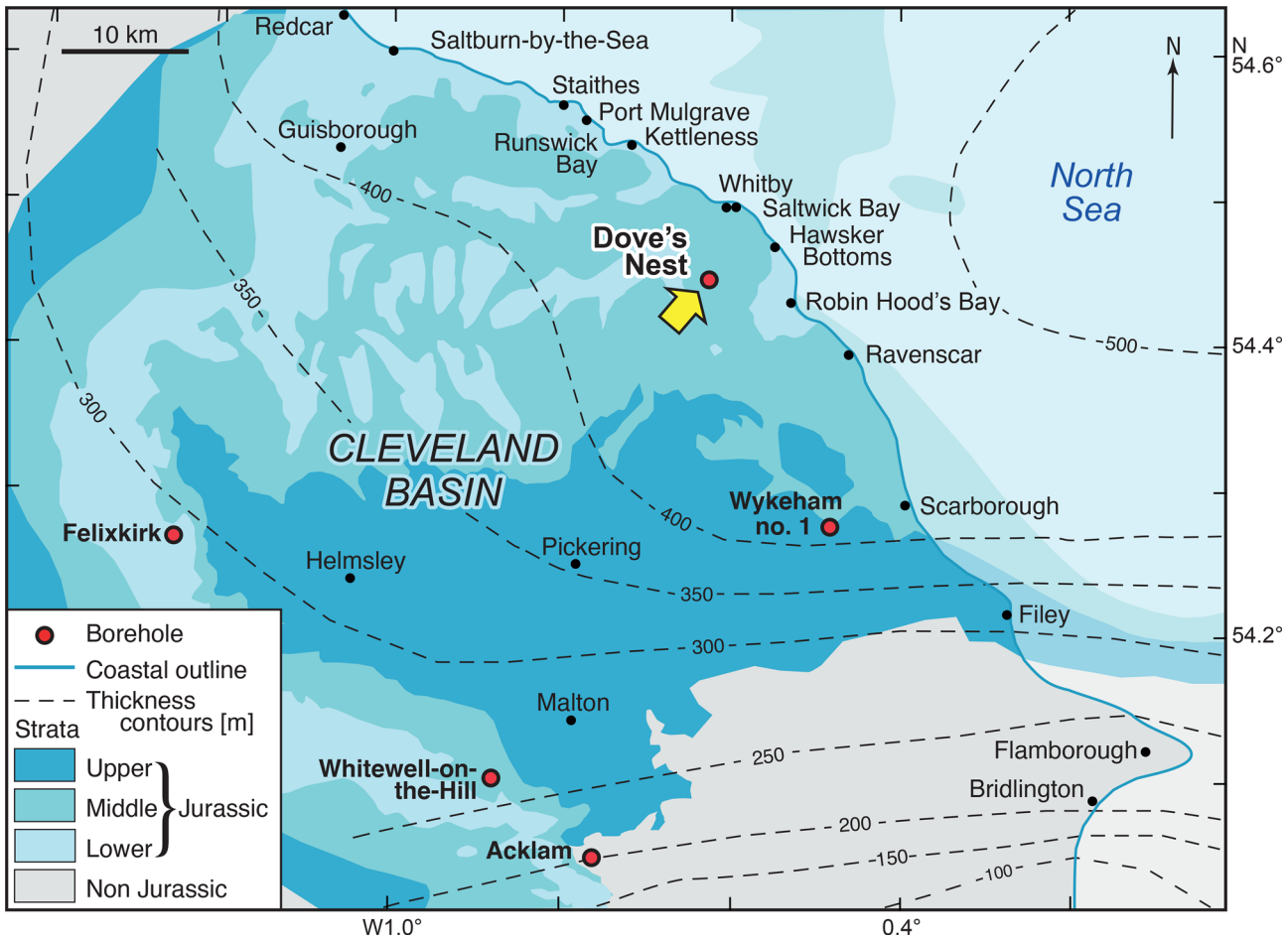

Fig. 1. Map of eastern North Yorkshire showing the geographic distribution of Jurassic sediments in the Cleveland Basin, isopachs for the Lias Group, and the location of Dove's Nest borehole (arrowed) and other relevant localities and boreholes mentioned in the text. Redrawn after Rawson and Wright (1995) and Kent (1980).

rocks at any given outcrop along the North Yorkshire coast. Nonetheless, the study of coastal outcrops still requires the measuring, sampling, and correlation of several sections along the coast, rather than working along a single vertical section as would be the case in a core. A previous core through the Lower Jurassic succession of Yorkshire has been described in the literature (viz., Ivimey-Cook and Powell 1991), the Felixkirk borehole (Fig. 1), but unfortunately the succession is condensed relative to the coast. Additionally, sedimentary rocks exposed in coastal outcrops, such as in North Yorkshire, are usually weathered, which may have affected the preservation of primary geochemical signals.

In 2013, an exploration borehole targeting Permian evaporites was drilled near Whitby, North Yorkshire, and a representative Jurassic succession was cored. The borehole was drilled farther north than existing boreholes, which are located to the south or west (Fig. 1), where the Lower Jurassic section is attenuated. Additionally, the new borehole was drilled closer to the classic coastal outcrops, which allows a more direct comparison to be made. The thickness of the middle and upper Lias Group (Staithes Sandstone, Cleveland Ironstone, and Whitby Mudstone formations) in the new core is approximately the same as that exposed on the North Yorkshire coast between Hawsker Bottoms and Whitby. However, unlike the rocks exposed along the North Yorkshire coast, the core represents a single, continuous vertical section through unweathered, immature Jurassic sediments that resembles those recovered by scientific drilling of younger oceanic crust.

We have studied the upper Pliensbachian to middle Toarcian part of the cored succession (Margaritatus to Bifrons zones). The studied succession is similar to that exposed between Hawsker Bottoms and Whitby (Fig. 1). Here, we describe the stratigraphy of the studied part of the core, correlate it to the coastal succession, and present a set of geochemical data that includes $\delta^{13}C_{org}$ values and total organic carbon (TOC) content.

Materials and methods

The Dove's Nest core

The Dove's Nest north shaft borehole (Fig. 1) was drilled in February 2013, by Fugro Geoservices UK, for Sirius Minerals, *c.* 5.5 km south of Whitby, North Yorkshire, England (UK National Grid: 489297, 505434). The drilling site is now the location of Woodsmith Mine.

We correlated the succession cored at Dove's Nest with the succession exposed along the Yorkshire coast on the basis of lithostratigraphy and $\delta^{13}C_{org}$ stratigraphy (Fig. 2). For our lithostratigraphic correlation, we used (i) Howarth's (1955) detailed section at Hawsker Bottoms, amended by Howarth (in Cope *et al.* 1980) and by Howard (1985); (ii) Howarth's (1973) detailed composite section of the Grey Shale Member, amended by Howarth (in Cope *et al.* 1980);

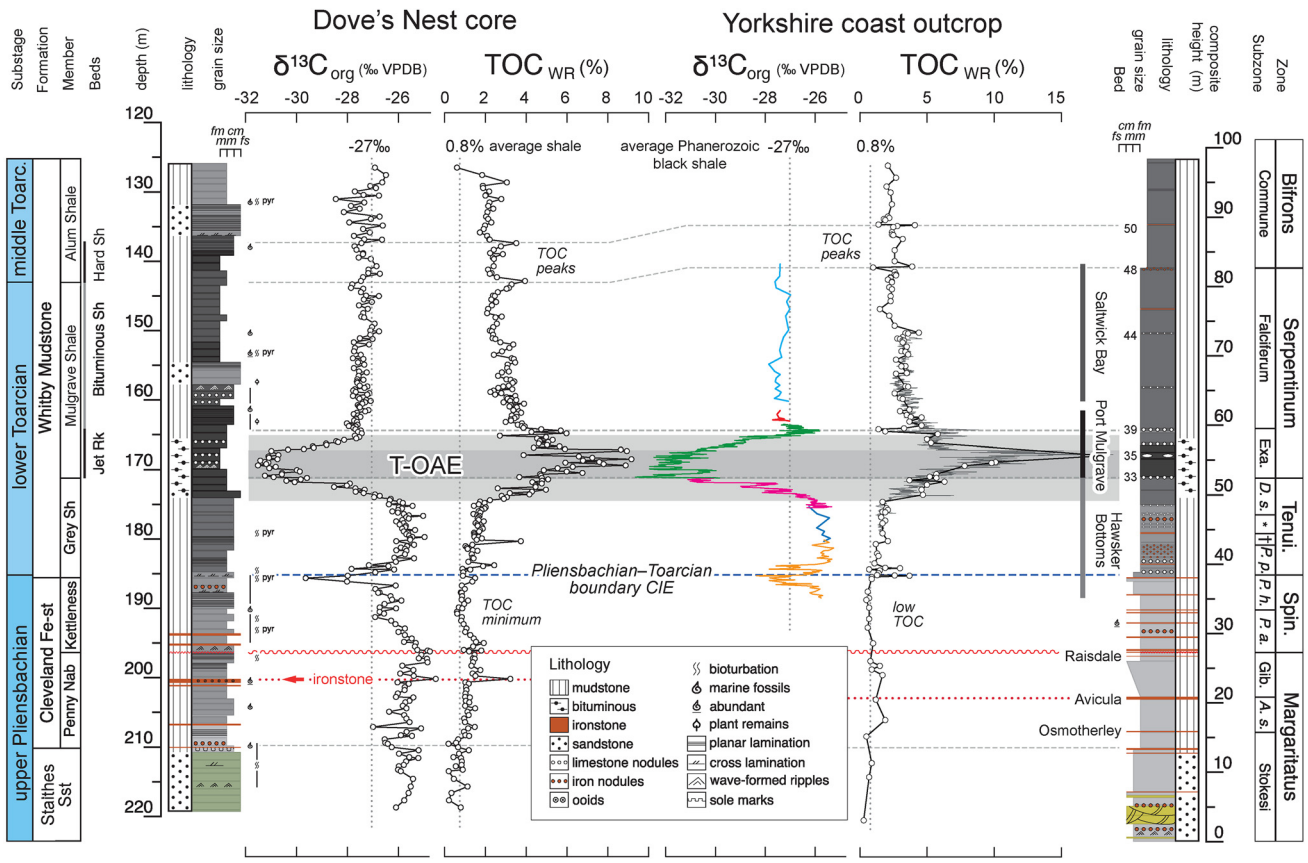

Fig. 2. Stratigraphic log of the studied section of Dove's Nest core (left) and of the correlative composite outcrop section along the North Yorkshire coast between Hawsker Bottoms and Port Mulgrave (right; Fig. 1). Organic carbon isotopes ($\delta^{13}C_{org}$) and whole-rock total organic carbon (TOC_{WR}) profiles are shown with their correlation. Grain size scale: fm, fine mudstone; mm, medium mudstone; cm, coarse mudstone; fs, very fine sandstone. Yorkshire coast 'bed' numbers from Port Mulgrave after Howarth (1962, 1992); named marker beds after Howarth (1955). Dove's Nest data from this study. Yorkshire coast $\delta^{13}C_{org}$ data from Hawsker Bottoms: orange, Littler *et al.* (2010); blue, Cohen *et al.* (2004); pink, Kemp *et al.* (2005). Port Mulgrave: green, Kemp *et al.* (2005); red, Cohen *et al.* (2004). Saltwick Bay: cyan, Cohen *et al.* (2004). TOC data for the Yorkshire coast are composite section values after McArthur (2019; thick line with unfilled circles) and Kemp *et al.* (2011; thin grey high-resolution curve). Abbreviations of biostratigraphic zonation: Tenui. = Tenuicostatum; Spin. = Spinatum; Exa. = Exaratum; *D. s.* = Semicelatum; * = Tenuicostatum; † = Clevelandicum; *P. p.* = Paltum; *P. h.* = Hawskerense; *P. a.* = Apyrenum; Gib. = Gibbosus; *A. s.* = Subnodosus.

(iii) Howarth's (1962) detailed sections at Rosedale Wyke, Port Mulgrave, and at Saltwick Nab; and (iv) Howarth's (1962) detailed section at Whitby, amended by Howarth (in Cope *et al.* 1980).

The studied succession (219.30–125.85 m) corresponds to the interval between 'bed' 7 (~'bed' 17 at Staithes harbour) in the Staithes Sandstone Formation at Castle Chamber, north of Robin Hood's Bay (Stokesi Subzone) and 'bed' 53 in the Alum Shale Formation at Whitby (Commune Subzone, Main Alum Shales). The core is from an essentially vertical borehole drilled normal to bedding with 100% recovery.

Our observations of the core were mostly made on the unsliced surface of the full barrel (e.g. Fig. 3a). Barrel diameter is 123 mm. At the top and bottom of core sections (three per box), we were able to observe the rocks on surfaces parallel to bedding (Fig. 3b–d). Where we took samples (see below), we were also able to study surfaces normal to bedding.

To describe the thickness of beds and laminae, we used the terminology proposed by Campbell (1967). In this paper, we use the term 'bed', between inverted commas, to refer to the finest stratigraphic subdivision of the middle and upper Lias of Yorkshire proposed by Howarth (1955, 1962), which has been subsequently used by most authors studying the succession (e.g. Hesselbo *et al.* 2000; Cohen *et al.* 2004; Kemp *et al.* 2005; Littler *et al.* 2010; Powell 2010; Thibault *et al.* 2018). We note, however, that these are neither genetic beds *sensu* Campbell (1967) nor geometric beds *sensu* McKee and Weir (1953).

Because the succession is mostly fine-grained, we adopted an approach modified from Lazar *et al.* (2015) to capture textural variability adequately using just a hand lens. Thus, here, we define fine mud as grains smaller than 10 μm, medium mud as grains between 10 and 30 μm, and coarse mud as grains between 30 and 62.5 μm. When fine mud dominates the fabric of a mudstone, the rock has a soap-like texture to the touch. Ten micrometres is approximately the boundary between the cohesive mud and sortable silt of McCave *et al.* (1995), as well as between (aggregate) grains that travel as bedload and grains that are brought into suspension by turbulence at the threshold of sediment movement. Grains between 10 and 30 μm cannot be resolved using a hand lens; however, when medium mud dominates the fabric of a mudstone, the rock feels gritty to the touch. Grains coarser than *c.* 30 μm are easily seen using a hand lens.

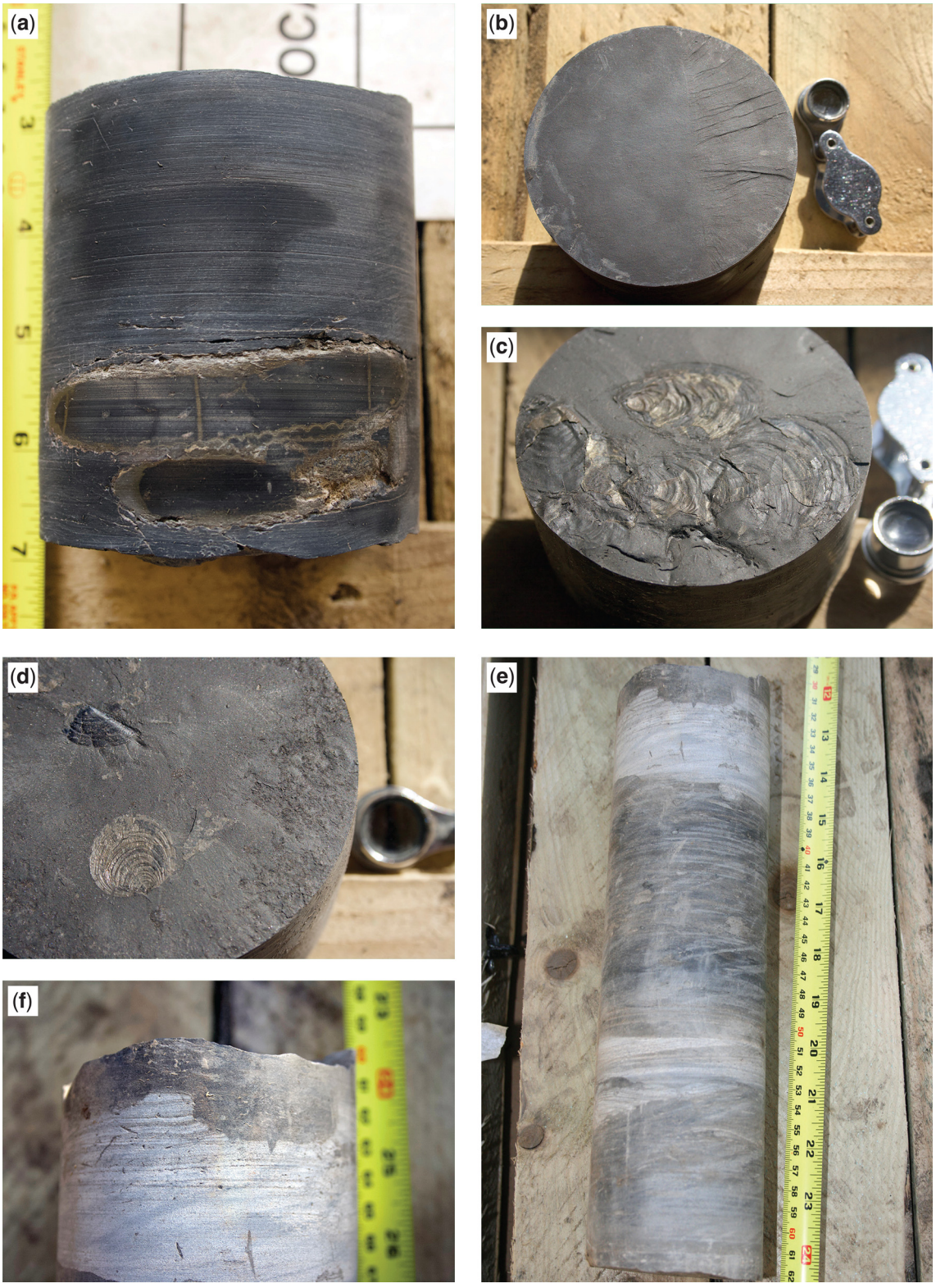

Fig. 3. Core photographs. Diameter of the core is 123 mm. (**a**) Uncompressed, mud-filled, pyrite-skinned dactylioceratid ammonite (*Dactylioceras cf. commune*) at 136.15 m in the Hard Shales (Alum Shale Member), (**b**) Homogeneous mudstone at 145.69 m in the Bituminous Shales (Falciferum Subzone), (**c**) Pyritized valves of *Pseudomytiloides dubius* at 161.30 m in the Bituminous Shales (Falciferum Subzone), (**d**) Pyritized valve of *Bositra buchi* (or *radiata*) and an ammonite aptychus at 172.50 m in the Grey Shale Member (Semicelatum Subzone), (**e**) 30 cm thick block (top: 186.20 m) showing two coarsening-upwards bedsets of dark grey coarse mudstone to blue-grey muddy sandstone in the Kettleness Member (Hawskerense Subzone). Bioturbation, though not intense, consists mostly of large *Chondrites*, (**f**) Detail of the top of block shown in (**e**) with dark grey mudstone above erosional surface cutting into blue-grey planar laminated and cross-laminated sandstone.

The rocks we studied in the fresh core were not fissile, because this property is developed after weathering. Therefore, we make no distinction between mudstones and shales. We use 'ironstone' to refer both to beds (seams) of (oolitic) ironstone and concretionary horizons of siderite. Sometimes we were able to observe the margins of a concretion, in which case we make a distinction between the two.

Sampling and analytical methods

In August and October 2013, we studied 93.45 m of the Dove's Nest core (north shaft) and collected a total of 280 samples at 20–50 cm intervals between 126.18 and 219.06 m depth. Each sample consisted of a quarter barrel slice about 0.5 cm thick. For this study, we took a chip with a mass of *c.* 1 g from each sample and ground it to a fine powder (*c.* 10 µm nominal diameter) using a Retsch agate mortar grinder (RM100).

Stable carbon isotope measurements of the bulk organic fraction were performed in the Stable Isotope Biogeochemistry Laboratory at Durham University, using a Costech elemental analyser (ESC 4010) coupled to a Thermo Scientific Delta V Advantage isotope ratio mass spectrometer. Ground bulk rock samples were decalcified overnight using a 3 M HCl solution in 50 ml centrifuge tubes. Carbon isotope ratios are corrected for ^{17}O contribution and reported in standard delta (δ) notation in per mil (‰) relative to Vienna Pee Dee belemnite (VPDB). Data accuracy was monitored through analyses of international and in-house standards calibrated against international standards (viz., IAEA 600, USGS 24, and USGS 40). Analytical uncertainty (2 standard deviations) for carbon isotope measurements was ±0.1 ‰ for replicate analyses of standards and <0.2 ‰ on replicate sample analyses. TOC of the insoluble residue was obtained as part of this method by using an internal standard (viz., glutamic acid; 40.82% C). Reproducibility of replicate samples was better than 0.2 wt% for TOC of the insoluble residue.

Calcium data were obtained by inductively coupled plasma-atomic emission spectrometry (ICP-AES) analysis of the samples using a JY Ultima 2C spectrometer at Kingston University London, UK. Samples were prepared following the lithium-metaborate fusion method of Jarvis (2003). By reference to international reference materials run with samples, accuracy and precision were judged to be <3%. We calculated calcium carbonate content using CaO data based on the assumption that all Ca resides in carbonate and used that result to calculate whole-rock TOC. The trends and values thus obtained generally agree closely with published whole-rock TOC values obtained from the coastal sections (Fig. 2).

Results

Core description

We studied the uppermost 9.15 m (upper Pliensbachian Stokesi Subzone) of the Staithes Sandstone Formation (bottom of studied interval: 219.3 m), which is *c.* 26 m thick at Castle Chamber, Robin Hood's Bay (and *c.* 29 m thick at Staithes harbour). In the core, the unit consists of blue-grey coarse mudstones and very fine sandstones. Cross-lamination and lenticular bedding are common. Coarser-grained beds are characterized by sharp erosional bases overlain by a laminated division that grades upward into a bioturbated division ('lam-scram' fabric of Warme 1991). We were able to identify low-angle *Planolites* and *Phycosiphon* burrows.

At the coast, east of Staithes, the sandstone beds of the Staithes Sandstone Formation, which weather yellow-brown, are characterized by low-angle cross-stratification, hummocky cross-stratification, and wave-formed ripples that are often embedded in mud drapes to produce wavy lamination. Farther south along the coast, closer to the location of the borehole, at Castle Chamber, the succession is finer-grained and the hummocky cross-stratified sandstone beds are not as thick or well developed as at Staithes. Similarly, in the core, there is more mud, the sandstones are finer and thinner, and the hummocky cross-stratified beds of the coastal exposures are missing.

The overlying upper Pliensbachian Cleveland Ironstone Formation is 24.59 m thick in the core (bottom: 210.15 m). Very thin to thin beds of grey medium to coarse mudstone dominate this interval. Beds have sharp erosional bases overlain by silt lags and are often bioturbated. At *c.* 210 m, 3 cm deep erosional sole marks (gutter casts) are present below an ironstone. We were able to identify five ironstone horizons in the lower 13.79 m of the unit (Penny Nab Member of Howard 1985); of these, the thickest and most prominent is at *c.* 200 m. This ironstone is particularly fossiliferous and its oolitic texture is prominent. We correlate it to the Avicula Seam at the top of the Subnodosus Subzone. The top of the Penny Nab Member correlates to the upper striped beds (Lower Gibbosus Shales). In the core, the upper striped beds appear as a succession of thin beds with erosional bedding planes and silt lags. Some of these structures are gutter casts (Greensmith *et al.* 1980). The Raisdale Seam, an ironstone between the Lower Gibbosus Shales and the Middle Gibbosus Shales (Cope *et al.* 1980), is either indistinct or absent in the core.

In the Dove's Nest core, as is the case in the individual coastal outcrops, the unconformable contact between the Margaritatus and Spinatum zones is indistinguishable from a bedding plane (i.e. it is a disconformity). Above the disconformity, the bottom of the Kettleness Member consists of a group of ironstone and mudstone beds referred to as the Pecten Seam. The bottom ironstone is oolitic, fossiliferous, and bioturbated, whereas the remaining two ironstone horizons are indistinct. At the coast, there is an additional ironstone horizon in the Pecten Seam; we could not see it in the core, however. The mudstones between the ironstone horizons vary between medium-grained and homogenous, with pyrite-filled small burrows, to coarser, thin-bedded, and (low-angle) cross-laminated. Coarse mudstones typically display lenticular bedding formed by starved combined-flow ripples of silt encased in finer mud. The top of the member (*c.* 187 m) is characterized by *Chondrites* above laminated mudstones (Fig. 3e, f). The Sulfur Band is not obvious in the core – probably due to the lack of weathering; Figure 4a, however, shows, in the core, the distinctive bioturbated layer (top 'bed' 43) that is also seen at Kettleness and Runswick above the Sulfur Band.

The mudstones of the Grey Shale Member (bottom: 185.57 m) are similar to those of the Cleveland Ironstone Formation with two key differences: they are a much darker grey and are not fossiliferous (but see Fig. 3d). This stratigraphic unit is the least fossiliferous of the studied core interval. Caswell and Coe (2014) described a very poorly fossiliferous interval at the top of the Grey Shale Member (their fig. 2). Conversely, the Cleveland Ironstone Formation and the Bituminous Shales (upper Mulgrave Shale Member, Falciferum Subzone), above the T-OAE $\delta^{13}C_{org}$

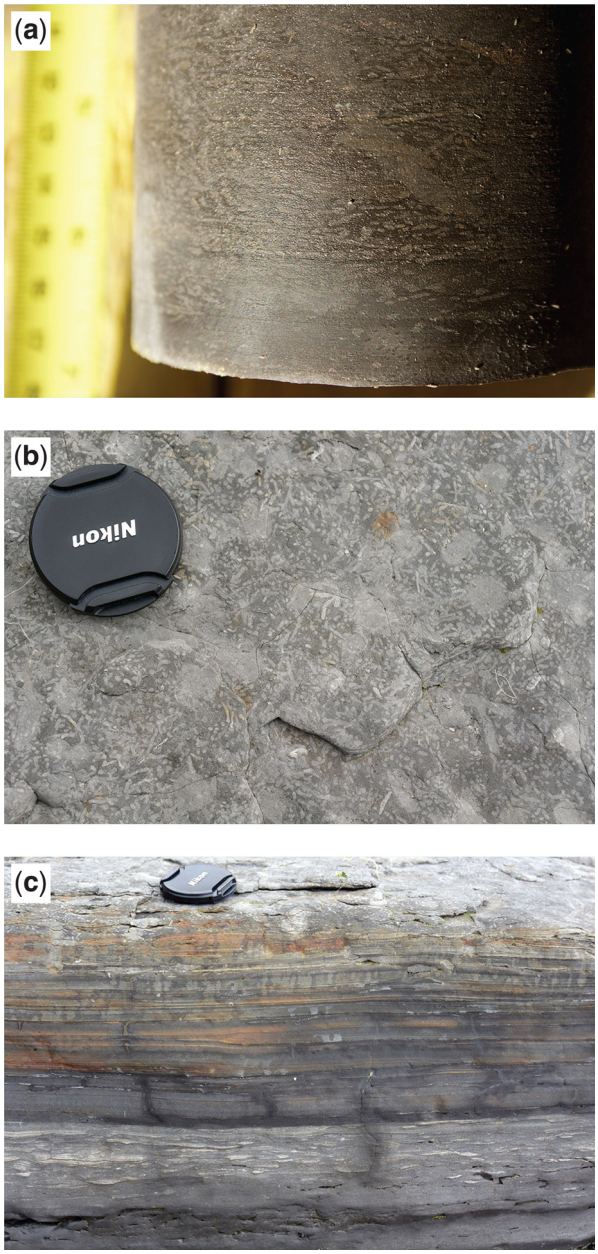

Fig. 4. Core and field photographs of the Pliensbachian-Toarcian boundary. (**a**) Core section between 185.05 and 184.91 m showing mudstone with abundant *Chondrites* and occasional *Teichichnus*, crosscut by later oblique *Rhizocorallium*(?), (**b**) Outcrop at the foot of the cliff at Kettleness a couple of metres below the Six Red Nodule Beds (Paltum Subzone). Coarsening upwards bedset of fine to coarse (ripple-)laminated mudstones above a coarsening upwards bedset showing lenticular heterolithic bedding. The top of the upper bedset is characterized by abundant *Chondrites*, (**c**) Detail of the top of the upper bedset shown in (**b**). Grey micaceous mudstone with abundant *Chondrites* exposed at the foot of the cliff at Kettleness. A similar exposure can be observed at the foot of the cliff of Brackenberry Wyke, between Staithes and Port Mulgrave (see Fig. 1).

negative excursion (Fig. 2), are the two most fossiliferous intervals of the core (Fig. 3c). We did not systematically collect body fossil data, however, and so we cannot distinguish between abundance and diversity. *Pseudomytiloides dubius* (Sowerby) (Fig. 3c), for example, can occur in very high-density monospecific assemblages (see Caswell and Coe 2014).

Towards the top of the Semicelatum Subzone, above *c.* 173 m, the mudstones of the Grey Shale Member become finer (claystone), darker, and rich in organic carbon (3–5% TOC compared to 1–2% below). Silt laminae, where present, are lenticular and thinner than below. This interval can be correlated to the top of 'bed' 31 at the coast (Fig. 2), where in addition to a similar change in texture, a decrease in terrigenous organic matter has been observed (French *et al.* 2014). The Exaratum Subzone (171.21–164.12 m), that is, the lowermost Mulgrave Shale Member (formerly known as the Jet Rock), continues the trend that started in the Semicelatum Subzone: the unit contains very little silt, and the black mudstones have a soap-like texture to the touch. This interval contains two horizons with nodules. We correlate the horizon at *c.* 169 m to the Whale Stones ('bed' 35).

Above the Jet Rock (*c.* 163 m), the Bituminous Shales (Mulgrave Shale Member) comprise thin beds of coarser mudstone with fossiliferous bedding planes characterized by monospecific assemblages of *P. dubius* (Fig. 3c). Cross-lamination reappears in these mudstones. The carbonaceous interval extends to about 158 m. The lower Bituminous Shales contain abrupt alternations of thin beds of fine and coarse mudstone that form striped beds. Towards the top of the unit, however, the mudstones are texturally similar to those of the Exaratum Subzone (Fig. 3b). Unlike the latter, they contain occasional very thin laminae of silt. The Bituminous Shales are fossiliferous, and rostra of belemnites are particularly common.

We studied the lower 17.95 m of the Alum Shale Member (bottom: 143.8 m). The lower part of the member, the Hard Shales, is similar to the striped beds of the lower Bituminous Shales. We place the bottom of the member based on the increase in $CaCO_3$ that defines the cementation characteristic of the Hard Shales. The Main Alum Shales (bottom: 137 m) above are very fine-grained and texturally similar to the mudstones of the Jet Rock.

There are some important lateral facies changes between the North Yorkshire coast and the core – namely, the Staithes Sandstone Formation is muddier in the core and not all ironstone horizons can be correlated between the coast and the core. The thickness of the middle and upper Lias Group formations in the core, however, is approximately the same as that exposed along the coast between Hawsker Bottoms and Whitby. In the Felixkirk borehole (Ivimey-Cook and Powell 1991), the thickness of the Cleveland Ironstone Formation is 9 m (Dove's Nest: 24.59 m) and the thickness of the Grey Shale and Mulgrave Shale members is 30.9 m (Dove's Nest: 41.77 m). Thus, unlike the Felixkirk borehole, the succession cored at Dove's Nest is not condensed relative to the North Yorkshire coast outcrops.

In the Dove's Nest core, the Bituminous Shales (Falciferum Subzone) are somewhat condensed relative to the section at Saltwick Nab and the Hard Shales (lower Commune Subzone) are a little expanded relative to the section at Whitby (Howarth 1962). At the coast the Bituminous Shales are 22.89 m thick and the Hard Shales are 6.32 m thick, whereas in the core the thickness of the units is 20.32 and 6.80 m.

Carbon isotope record and TOC

Here, we present the first $\delta^{13}C_{org}$ record obtained from a single vertical section between the Margaritatus and Bifrons

zones ('beds' 7 to 53) in the Cleveland Basin. This interval includes the top of the Staithes Sandstone Formation; the Cleveland Ironstone Formation; and the Grey Shale, Mulgrave Shale, and bottom of the Alum Shale members of the Whitby Mudstone Formation.

A $\delta^{13}C_{org}$ negative excursion starts at 196.27 m, at the base of the Spinatum Zone, above the disconformity that separates the Penny Nab and Kettleness members of the Cleveland Ironstone Formation. This negative excursion, the Pliensbachian–Toarcian Boundary Event (Cramer and Jarvis 2020), culminates in a complex negative excursion at the Pliensbachian–Toarcian boundary (see Littler *et al.* 2010). At the resolution of our sampling for this part of the core, we observe two negative excursions: a lower larger negative excursion (3.5 ‰ $\delta^{13}C_{org}$) between 186.83 and 185.75 m and an upper smaller and thinner negative excursion (1.7 ‰ $\delta^{13}C_{org}$) between 184.51 and 184.41 m. Recovery from this complex negative excursion, that is, a return to pre-excursion values, is achieved at 182.88 m.

'Beds' 31–34 of the Grey Shale and lower Mulgrave Shale members (174.83–169.39 m) contain the large $\delta^{13}C_{org}$ negative excursion (5.7 ‰ $\delta^{13}C_{org}$) that is normally used to define the T-OAE (Fig. 2; Hesselbo *et al.* 2000). Recovery from the negative excursion, that is, a return to less ^{13}C-depleted values is achieved at 165.31 m. We find, however, no evidence for a $\delta^{13}C_{org}$ positive excursion in 'beds' 38–41 immediately above the T-OAE (cf. Hesselbo *et al.* 2000; Kemp *et al.* 2005). Additionally, our record does not show a longer-term $\delta^{13}C_{org}$ positive excursion thought to be interrupted by the T-OAE negative excursion. Rather, we observe that $\delta^{13}C_{org}$ values below the T-OAE negative excursion (average: −25.9 ‰) are consistently less ^{13}C-depleted than those above it (average: −27.5 ‰). This distinctive step down in $\delta^{13}C_{org}$ values may reflect a change from more terrestrial dominated organic matter below the excursion to more marine dominated organic matter above (see French *et al.* 2014, for example). This is the opposite of what has been observed in Peniche and Sancerre, where post-excursion values in *carbonate* carbon isotopes ($\delta^{13}C_{carb}$) are higher than pre-excursion values (Hesselbo *et al.* 2007; Hermoso *et al.* 2009).

A comparable trend can be observed in TOC values (see also Table 1): below the T-OAE negative excursion values are lower (average: 1.3%) than above it (average: 3.1%). Using TOC values, we can subdivide the studied succession into four parts (Fig. 2). Below the T-OAE negative excursion, there are two sequences in each of which TOC values increase upwards. The lower sequence up to *c.* 195 m, near the top of the Penny Nab Member, and the upper sequence up to *c.* 174.5 m, in the Semicelatum Subzone, at the onset of the T-OAE as defined using $\delta^{13}C_{org}$ (but see Them *et al.* 2018 who argued for a longer interval of oceanic anoxia starting at the Pliensbachian–Toarcian boundary). Maximum TOC values (≥6%) are reached between *c.* 170.5 and *c.* 167 m with two distinct peaks: the lower, larger peak coincides with 'bed' 35 and the upper peak with the top of 'bed' 38. Above this 'bed', values decrease slowly upwards.

Table 1. *Summary of the composition of the studied samples (see Supplementary materials for full datasets)*

Formation	Member	$CaCO_3$	TOC_{WR}
Whitby Mudstone	Alum Shale	**0.6**; 0.2–65.6	**2.2**; 0.6–3.5
	Mulgrave Shale (including the Jet Rock)	**5.9**; 0.5–81.3	**3.3**; 2.1–9.2
	Jet Rock (Exaratum Subzone)	**10.3**; 1.7–81.3	**5.5**; 2.7–9.2
	Grey Shale	**2.9**; 0.6–9.3	**1.7**; 0.9–5.1
Cleveland Ironstone	Kettleness	**0.7**; 0.1–11.9	**1.0**; 0.6–1.9
	Penny Nab	**0.6**; 0.1–13.5	**1.2**; 0.2–3.2
Staithes Sandstone		**1.1**; 0.3–17.2	**0.7**; 0.2–1.2

Median values are in bold and the minimum to maximum range in roman. All data are reported in weight per cent and rounded to 1 decimal point.

Discussion

Stratigraphic issues in the upper Pliensbachian

Along the North Yorkshire coast, the Staithes Sandstone Formation grades upwards into the Cleveland Ironstone Formation. The top of the former is similar to coarser intervals of the latter; the lower striped beds, for example, are a slightly coarser version of the upper striped beds. In the studied core, the Staithes Sandstone Formation is finer and, towards its top, difficult to distinguish from the overlying Cleveland Ironstone Formation. Howarth (in Cope *et al.* 1980) and Powell (1984) placed the base of the Cleveland Ironstone Formation at the base of 'beds' 14 and 12, respectively. Howard (1985) placed it at the base of 'bed' 17, at the base of the lowest coarsening-upward cycle, and we follow his placement (see de Vos 2017). In the Felixkirk borehole, the Osmotherley Seam rests directly on the Staithes Sandstone Formation with no intervening mudstone (Powell 1984).

The contact between the Margaritatus and Spinatum zones (196.36 m), that is, between 'beds' 24 and 25, is a disconformity that represents the eroded upper part of the Gibbosus Subzone; here, the uppermost Middle Gibbosus Shales, the Two-foot Seam, and the Upper Gibbosus Shales are missing (see fig. 24 in Chowns 1968). Unlike at Staithes, however, the bottom of the Spinatum Zone (Pecten Seam) is complete (see fig. 9 in Cope *et al.* 1980). At the scale of the basin, however, the contact is clearly an angular unconformity (see fig. 26 in Chowns 1968). Even though the contact

Fig. 5. Field photograph of the upper 'bed' 31 (Grey Shale Member) at Kettleness (diameter of coin: 23.4 mm). The grey mudstones encase more indurated laminasets of coarse siltstone and very fine to medium sandstone that show intricately interwoven cross-lamination.

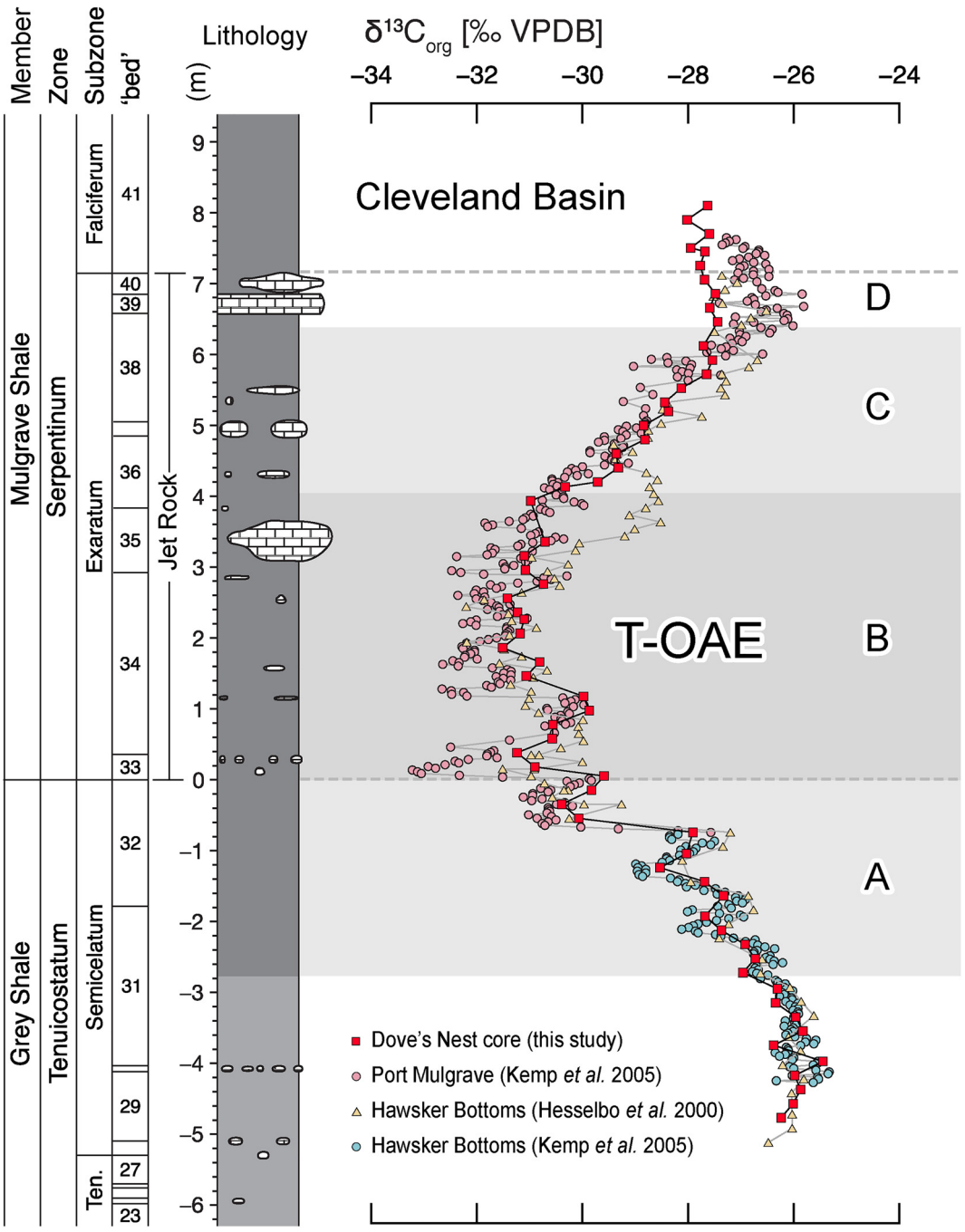

Fig. 6. Comparison of the organic carbon isotope records of the Toarcian Oceanic Anoxic Event in the Cleveland Basin. Stratigraphic log of 'beds' 23–41 modified from Kemp *et al.* (2005). Blue circles represent data from Hawsker Bottoms and pink circles represent data from Port Mulgrave by Kemp *et al.* (2005). Yellow triangles represent data from Hawsker Bottoms by Hesselbo *et al.* (2000). Red squares represent data from the Dove's Nest core (this study). Between 'beds' 29 and 32, the three records are similar. In 'beds' 33 and 34, the record of Kemp *et al.* (2005) shows consistently more ^{13}C-depleted values than the other two records. In 'beds' 35 and 36, the record of Hesselbo *et al.* (2000) shows a small positive excursion that is absent in the other two records. In our record, recovery from the negative excursion is achieved in 'bed' 38 (cf. Fig. 2). Thus, unlike in the other two records, there is no small positive excursion in 'beds' 39 and 40 in our data.

becomes a nonsequence (diastem) towards the north, in much of the Cleveland Basin – and in the Dove's Nest core – the contact is unconformable.

The top of the Kettleness Member (*c.* 187 m) is characterized by *Chondrites* above laminated mudstones (Fig. 3e, f). These can also be observed immediately below the Sulfur Band in the coastal exposures east-SE of Staithes (Fig. 4b, c). The Pliensbachian–Toarcian boundary is thus placed above the *Chondrites* interval at 185.19 m. This placement of the Pliensbachian–Toarcian boundary is in agreement with the $\delta^{13}C_{org}$ record (Littler *et al.* 2010): we observe a negative excursion below the boundary (185.75 m) and a second negative excursion above it (184.41 m) (Fig. 2).

Howarth (1973 and in Cope *et al.* 1980) and Powell (1984) assigned 'beds' 43 and 44 to the Cleveland Ironstone Formation. According to this placement, the Pliensbachian–Toarcian boundary falls within the Kettleness Member, and many authors have followed this convention (e.g. McArthur *et al.* 2008; Littler *et al.* 2010; Thibault *et al.* 2018; Hesselbo and King 2019). These 'beds' consist of carbonaceous mudstone interbedded with coarse mudstone and calcareous nodules, which are characteristic of the overlying Grey Shale

Member. For this reason, Howard (1985) proposed that these 'beds' be assigned to the Grey Shale Member and that the base of the member be lowered to the top of 'bed' 42. 'Bed' 43 contains the base of the Paltum Subzone and of the Toarcian. We have followed his proposal. Thus, instead of placing the bottom of the Grey Shale Member at 184.81 m, we placed it at 185.57 m, 38 cm below the Pliensbachian–Toarcian boundary.

Sedimentology of the lower Toarcian

In the Grey Shale Member at Kettleness, about a metre below the Cannonball Doggers, Wignall *et al.* (2005) described an interval of beds with erosional bases, up to 3 cm relief, consisting of medium mudstones with coarse silt laminae and hummocky cross-stratified (HCS) sand (up to medium-grained). They noted that this interval corresponds to the mudstones with current lamination features of O'Brien (1990). The structures in this interval (Fig. 5), which they called the 'HCS zone', resemble the 'intricately interwoven cross-lamination' of de Raaf *et al.* (1977; see their fig. 8). Trabucho-Alexandre (2015; his fig. 6f) described combined-flow ripples from this interval at Port Mulgrave that resemble the sedimentary structures found in the laminated silt-streaked mudstones of the lower and upper striped beds of the underlying Staithes Sandstone and Cleveland Ironstone formations at Jet Wyke (Chowns 1968; Greensmith *et al.* 1980). In addition to thick silt laminasets, the striped beds are characterized by scour marks (gutters) cut into then already consolidated mud and filled with normally graded laminated coarse mud.

O'Brien (1990) described an alternation of thick and wavy lamination in the Grey Shale Member and the Jet Rock (lower Mulgrave Shale Member) at Port Mulgrave, which he interpreted as wave-formed and benthic microbial mat structures, respectively. Wavy laminated intervals show evidence for reworking by storms. French *et al.* (2014) reported the aromatic carotenoid derivative, okenone, from the wavy laminated interval and interpreted its sedimentary source to have been microbial mats. Okenone requires extremely shallow photic-zone euxinia and a highly restricted environment. Water-depth at the time of deposition is estimated to have been a few tens of metres (Hallam 1975; Trabucho-Alexandre *et al.* 2012; French *et al.* 2014; Trabucho-Alexandre 2015), which means that the seafloor was well within the photic zone.

In the Dove's Nest core, the mudstones of the Exaratum Subzone are finer than those studied by previous authors (e.g. O'Brien 1990) farther north in the Cleveland Basin, and may represent sedimentation in a deeper part of the basin. The top of the Jet Rock ('bed' 39) and the lowermost Bituminous Shales, however, are similar to the mudstones described by O'Brien (1990) and contain thin beds of cross-laminated coarse mudstone that give the core a striped aspect.

Sedimentary evidence from lower Toarcian mudstones in the Cleveland Basin suggests that the seafloor was above storm wave-base during deposition of the Grey Shale Member and that storm-driven bottom currents were responsible for much sediment erosion, transport, and deposition during the interval of oceanic anoxia, when the Grey Shale and the lower (Exaratum Subzone) Mulgrave Shale members were deposited (O'Brien 1990; Wignall *et al.* 2005; Ghadeer and Macquaker 2011, 2012; Trabucho-Alexandre 2015). Similar evidence has been reported from the Dutch Central Graben, another basin in the northern Laurasian Sea (Trabucho-Alexandre *et al.* 2012). Lower Jurassic sediments deposited in the shallower parts of the northern Laurasian Sea (viz., platforms and highs), where the impact of storms on sedimentation would have been even greater, were removed by erosion during the middle and late Cimmerian uplift (Wong 2007).

The Laurasian Sea was a hurricane-dominated region and the greenhouse climate of the Early Jurassic allowed hurricanes to form and intensify at higher latitudes than at present (see Studholme *et al.* 2022). Hurricanes dominate the western margins of major oceans; the Tethys, with its high sea-surface temperatures, large generating area, and long overwater path towards Pangaea, was ideal for hurricane generation (see Marsaglia and Klein 1983). As a result of more intense tropical storms, in the early Toarcian, storm wave-base appears to have been deeper than at present (Krencker *et al.* 2015).

Ghadeer and Macquaker (2012) suggested that storms in the Laurasian Sea promoted rapid organic carbon burial and, thus, contributed to its preservation. März *et al.* (2016) and Tribovillard *et al.* (2019) proposed mechanical concentration of sulfurized organic carbon as a mechanism to explain elevated organic carbon content in shallow-marine mudstones characterized by sedimentary structures attributed to storms. In the case of the Laurasian Sea, the source of organic carbon, as well as okenone (French *et al.* 2014), was perhaps the extremely shallow seafloor of platforms and highs (e.g. Market Weighton; Wright 2022), where a form of dynamic bypassing resulted in stratigraphic condensation on the platform and the concentration of (carbonaceous) sediment into the subsiding basins (Hallam and Sellwood 1976; Jenkyns and Macfarlane 2022; and see fig. 8 in Wignall *et al.* 2005).

Above 'bed' 42, the mudstones become similar to those of the Exaratum Subzone but with fine silt laminae, which were probably produced by ripples migrating on the seafloor (Yawar and Schieber 2017). The same trend was observed at Port Mulgrave (O'Brien 1990). The top of the Mulgrave Shale Member shows a fining-upwards trend. The finest mudstones in the succession, which probably reflect maximum flooding and the deepest water conditions in the basin, below storm wave-base, occur in the middle of the Alum Shale Member (Pye and Krinsley 1986), that is, in the middle Toarcian (lower Bifrons Zone).

Carbon isotope record and TOC

The extant $\delta^{13}C_{org}$ record of Yorkshire consists of a composite of datasets by Cohen *et al.* (2004), Kemp *et al.* (2005), Littler *et al.* (2010), and, more recently, Thibault *et al.* (2018) and Van de Schootbrugge *et al.* (2020). Cohen *et al.* (2004) analysed samples from the Tenuicostatum to lowermost Bifrons zones; their data are a composite from Hawsker Bottoms, Port Mulgrave, and Saltwick Bay. Littler *et al.* (2010) analysed samples from the Spinatum and Tenuicostatum zones (Pliensbachian–Toarcian boundary). Kemp *et al.* (2005) analysed samples from the Tenuicostatum

and lower Serpentinum zones (T-OAE); their data are a composite from Hawsker Bottoms and Port Mulgrave spliced at 'bed' 33 (Fig. 2). Thibault *et al.* (2018) analysed samples from the Serpentinum and Bifrons zones. We did not include the data of Thibault *et al.* (2018) in Figure 2 because it is a small dataset, mostly in the Bituminous Shales, with some uncertainty concerning the splice. Van de Schootbrugge *et al.* (2020) analysed samples at low resolution between the Davoei and Thouarsense zones. Their data are also not easily spliced with the remainder of the data and are, therefore, not included here either. These difficulties illustrate the advantages of obtaining chemostratigraphic data from a single, continuous vertical section (see Gröcke 2020).

There are two chief differences between our longer continuous record and previously published records: (1) We observe a negative trend, starting at 196.18 m, at the base of the Spinatum Zone, above the disconformity that separates the Penny Nab and Kettleness members (cf. Storm *et al.* 2020). This negative trend culminates in the complex $\delta^{13}C_{org}$ negative excursion at the Pliensbachian–Toarcian boundary described by Littler *et al.* (2010). (2) We find no evidence for a $\delta^{13}C_{org}$ positive excursion in 'beds' 38–41 immediately above the T-OAE (cf. Hesselbo *et al.* 2000; Kemp *et al.* 2005). Additionally, our record does not show a longer-term $\delta^{13}C_{org}$ positive excursion that is interrupted by the T-OAE negative excursion (cf. our Fig. 2 with fig. 4 in Jenkyns *et al.* 2001, fig. 1 in Them *et al.* 2018, and fig. 2 in Storm *et al.* 2020).

The thickness of the T-OAE negative excursion in the Dove's Nest core is the same as that of the curves of Hesselbo *et al.* (2000) and Kemp *et al.* (2005), which come from the lower Toarcian outcrops at Hawsker Bottoms and Port Mulgrave on the North Yorkshire coast (Fig. 6). The shape of the excursion is similar to that of Kemp *et al.* (2005), but the absolute values are less ^{13}C-depleted and, thus, similar to those of Hesselbo *et al.* (2000).

In 'beds' 32–34, our record contains the three abrupt $\delta^{13}C_{org}$ shifts attributed by Kemp *et al.* (2005) to pulses of methane release and by Trabucho-Alexandre (2015) to erosion. This – or, at least, a *very* similar – abruptly stepped morphology of the δ^{13}C record is also clearly present in the Sancerre core, Paris Basin (Hermoso *et al.* 2009, 2012), and in the Mochras core, Cardigan Bay Basin (Jenkyns *et al.* 2001; Xu *et al.* 2018; Storm *et al.* 2020), which suggests that the process responsible for the abrupt shifts is at least regional. Farther east, steps have also been observed in coastal and marginal marine successions in the Polish Basin (Hesselbo and Pieńkowski 2011), but the morphology of the δ^{13}C record is different enough that correlation of the steps requires an assumption that the steps can be correlated.

If the three abrupt shifts represent pulses of methane release, then we would expect to observe a similar stepped morphology in many if not most records – in those that are complete. This, however, does not appear to be the case. In Peniche, Lusitanian Basin, for example, only one abrupt shift can be recognized (Hesselbo *et al.* 2007). In Haida Gwaii, British Columbia, Canada, the negative excursion is bound by two abrupt shifts but no stepwise excursion can be observed (Caruthers *et al.* 2011; Them *et al.* 2017). In the East Tributary of Bighorn Creek, Alberta, abrupt shifts in the δ^{13}C record are associated with bedding planes of sandstone beds and surfaces where carbonate content changes (Them *et al.* 2017). In both western North American examples, there are also abrupt shifts in the other direction, that is, towards less ^{13}C-depleted values (see fig. 2 in Caruthers *et al.* 2011; and fig. 2 in Them *et al.* 2017). It is clear that both stratigraphic sections and their δ^{13}C records represent an incomplete record of the T-OAE, particularly of the lower, falling limb.

Here, we do not question the input of isotopically light carbon into the ocean–atmosphere system. We also do not question that, during the T-OAE, there were (short) phases of environmental rebound that resulted in δ^{13}C trends towards less ^{13}C-depleted values. Rather, we argue that the abrupt shifts (A–C *sensu* Kemp *et al.* 2005) in the δ^{13}C record are an artefact of erosive processes and do not represent geologically abrupt input of carbon from an extremely ^{13}C-depleted carbon source. Thus, the finer morphology of the δ^{13}C record cannot be used to infer the timescale of the processes driving the carbon cycle perturbation during the T-OAE.

Heimdal *et al.* (2021) have shown that a source of extremely ^{13}C-depleted carbon, such as methane clathrates, is not required to replicate the T-OAE negative excursion. Gröcke *et al.* (2009) also argued against another methane hypothesis (thermogenic methane), showing that igneous intrusions would not have the energy to produce the amount of methane gas required to cause the T-OAE $\delta^{13}C_{org}$ negative excursion.

The simplest explanation for the abrupt shifts observed in δ^{13}C records of the lower Toarcian is erosion (by storms) that resulted in nonsequences (diastems) that affect the morphology of the δ^{13}C record (see fig. 9 in Trabucho-Alexandre 2015; Them *et al.* 2017; Gröcke 2020). On the scale of the Laurasian Sea, some of these erosional surfaces might therefore be useful for correlation (see also Pittet *et al.* 2014).

Conclusions

The studied interval of the Dove's Nest core contains a nearly complete upper Pliensbachian–middle Toarcian succession similar to that exposed along the North Yorkshire coast between Hawsker Bottoms and Whitby ('beds' 7 to 53). We place the Pliensbachian–Toarcian boundary at 185.19 m depth.

The core contains the complex $\delta^{13}C_{org}$ negative excursion at the Pliensbachian–Toarcian boundary (between 186.83 and 182.88 m) and the negative excursion (5.7 ‰ $\delta^{13}C_{org}$) in the lower Toarcian (174.83–165.31 m) that represents the T-OAE. We found no evidence for a longer-term $\delta^{13}C_{org}$ positive excursion in the lower Toarcian.

The Middle Gibbosus Shales, Two-foot Seam, and the Upper Gibbosus Shales are missing in a disconformity at 196.36 m. The bottom of the Spinatum Zone, however, is complete, unlike at Staithes.

Sedimentary structures in the lower Toarcian suggest that the seafloor was above storm wave-base and that storm-driven bottom currents were responsible for much sediment erosion, transport, and deposition during the interval of oceanic anoxia. The abrupt shifts observed in the $\delta^{13}C_{org}$ record are likely to reflect the impact of erosion by storms on the morphology of the δ^{13}C record of the T-OAE.

Acknowledgements We thank Anglo American Woodsmith Project (formerly Sirius Minerals) for allowing us to study and sample the core; Howard Armstrong for helping us describe and sample the core; Chris Dalby and Kate Olde for assistance during work in the laboratory; Andrew Caruthers for identifying the ammonite in Figure 3a; Martin Aberhan for identifying the fossils in Figure 3d; Juergen Schieber for identifying the sedimentary structure in Figure 5; and Stephen Hesselbo, Paul Wignall, and an anonymous reviewer for their comments on an earlier version of this manuscript.

Author contributions **JPT-A**: conceptualization (equal), data curation (lead), formal analysis (lead), methodology (equal), writing – original draft (lead), writing – review & editing (lead); **DRG**: formal analysis (supporting), funding acquisition (equal), methodology (equal), writing – review & editing (supporting); **EA**: formal analysis (supporting), writing – review & editing (supporting); **LH**: conceptualization (equal), formal analysis (supporting), writing – review & editing (supporting); **IJ**: funding acquisition (equal), methodology (supporting), writing – review & editing (supporting)

Funding DRG and IJ acknowledge funding by UK Natural Environment Research Council (NERC) grants NE/H021868/1 and NE/H020756/1, respectively, which made the analytical work presented here possible.

Competing interests The authors declare that they have no known competing financial interests or personal relationships that could have appeared to influence the work reported in this paper.

Data availability All data generated or analysed during this study are included in this published article (and its supplementary information files).

Scientific editing by Jed Atkinson and Paul Wignall

References

Adrichem Boogaert, H.A.van and Kouwe, W.F.P. 1993–1997. *Stratigraphic Nomenclature of The Netherlands: Revision and Update by RGD and NOPEGA*. *Mededelingen Rijks Geologische Dienst*, **50**.

Baroni, I.R., Pohl, A. *et al.* 2018. Ocean circulation in the Toarcian (Early Jurassic): a key control on deoxygenation and carbon burial on the European shelf. *Paleoceanography and Paleoclimatology*, **33**, 994–1012, https://doi.org/10.1029/2018PA003394

Campbell, C.V. 1967. Lamina, laminaset, bed and bedset. *Sedimentology*, **8**, 7–26, https://doi.org/10.1111/j.1365-3091.1967.tb01301.x

Caruthers, A.H., Gröcke, D.R. and Smith, P.L. 2011. The significance of an Early Jurassic (Toarcian) carbon-isotope excursion in Haida Gwaii (Queen Charlotte Islands), British Columbia, Canada. *Earth and Planetary Science Letters*, **307**, 19–26, https://doi.org/10.1016/j.epsl.2011.04.013

Caswell, B.A. and Coe, A.L. 2012. A high-resolution shallow marine record of the Toarcian (Early Jurassic) Oceanic Anoxic Event from the East Midlands Shelf, UK. *Palaeogeography, Palaeoclimatology, Palaeoecology*, **365–366**, 124–135, https://doi.org/10.1016/j.palaeo.2012.09.021

Caswell, B.A. and Coe, A.L. 2014. The impact of anoxia on pelagic macrofauna during the Toarcian Oceanic Anoxic Event (Early Jurassic). *Proceedings of the Geologists' Association*, **125**, 383–391, https://doi.org/10.1016/j.pgeola.2014.06.001

Chowns, T.M. 1968. *Environmental and Diagenetic Studies of the Cleveland Ironstone Formation of North East Yorkshire*. PhD dissertation, University of Newcastle upon Tyne, http://theses.ncl.ac.uk/jspui/handle/10443/268

Cohen, A.S., Coe, A.L., Harding, S.M. and Schwark, L. 2004. Osmium isotope evidence for the regulation of atmospheric CO_2 by continental weathering. *Geology*, **32**, 157–160, https://doi.org/10.1130/G20158.1

Cope, J.C.W., Getty, T.A., Howarth, M.K., Morton, N. and Torrens, H.S. 1980. *A Correlation of Jurassic Rocks in the British Isles. Part One: Introduction and Lower Jurassic*. *Geological Society, London, Special Report*, **14**.

Cramer, B.D. and Jarvis, I. 2020. Chapter 11 - Carbon isotope stratigraphy. *In:* Gradstein, F.M., Ogg, J.G., Schmitz, M.D. and Ogg, G.M. (eds) *Geologic Time Scale 2020*. Elsevier, Amsterdam, 309–343, https://doi.org/10.1016/B978-0-12-824360-2.00011-5

de Raaf, J.F.M., Boersma, J.R. and van Gelder, A. 1977. Wave-generated structures and sequences from a shallow marine succession, Lower Carboniferous, County Cork, Ireland. *Sedimentology*, **24**, 451–483, https://doi.org/10.1111/j.1365-3091.1977.tb00134.x

de Vos, L. 2017. *Textural and Mineralogical Characterization of the Late Pliensbachian-Early Toarcian Sediments of the Cleveland Basin, Yorkshire, U.K.* Master's dissertation, Universiteit Utrecht, https://studenttheses.uu.nl/handle/20.500.12932/28170

French, K.L., Sepúlveda, J., Trabucho-Alexandre, J., Gröcke, D.R. and Summons, R.E. 2014. Organic geochemistry of the early Toarcian oceanic anoxic event in Hawsker Bottoms, Yorkshire, England. *Earth and Planetary Science Letters*, **390**, 116–127, https://doi.org/10.1016/j.epsl.2013.12.033

Ghadeer, S.G. and Macquaker, J.H.S. 2011. Sediment transport processes in an ancient mud-dominated succession: a comparison of processes operating in marine offshore settings and anoxic basinal environments. *Journal of the Geological Society*, **168**, 1121–1132, https://doi.org/10.1144/0016-76492010-016

Ghadeer, S.G. and Macquaker, J.H.S. 2012. The role of event beds in the preservation of organic carbon in fine-grained sediments: analyses of the sedimentological processes operating during deposition of the Whitby Mudstone Formation (Toarcian, Lower Jurassic) preserved in northeast England. *Marine and Petroleum Geology*, **35**, 309–320, https://doi.org/10.1016/j.marpetgeo.2012.01.001

Greensmith, J.T., Rawson, P.F. and Shalaby, S.E. 1980. An association of minor fining-upward cycles and aligned gutter marks in the Middle Lias (lower Jurassic) of the Yorkshire Coast. *Proceedings of the Yorkshire Geological Society*, **42**, 525–538, https://doi.org/10.1144/pygs.42.4.525

Gröcke, D.R. 2020. Carbon isotope stratigraphy: principles and applications. *In:* Montenari, M. (ed.) *Stratigraphy & Timescales*. *Carbon Isotope Stratigraphy*, **5**, 1–40, https://doi.org/10.1016/bs.sats.2020.08.002

Gröcke, D.R., Rimmer, S.M., Yoksoulian, L.E., Cairncross, B., Tsikos, H. and van Hunen, J. 2009. No evidence for thermogenic methane release in coal from the Karoo-Ferrar large igneous province. *Earth and Planetary Science Letters*, **277**, 204–212, https://doi.org/10.1016/j.epsl.2008.10.022

Hallam, A. 1975. *Jurassic Environments*. Cambridge Earth Science Series. Cambridge University Press, Cambridge.

Hallam, A. and Sellwood, B.W. 1976. Middle Mesozoic sedimentation in relation to tectonics in the British area. *The Journal of Geology*, **84**, 301–321, https://doi.org/10.1086/628197

Heimdal, T.H., Goddéris, Y., Jones, M.T. and Svensen, H.H. 2021. Assessing the importance of thermogenic degassing from the Karoo Large Igneous Province (LIP) in driving Toarcian carbon cycle perturbations. *Nature Communications*, **12**, 6221, https://doi.org/10.1038/s41467-021-26467-6

Hemingway, J.E. 1974. Jurassic. *In:* Rayner, D.H. and Hemingway, J.E. (eds) *The Geology and Mineral Resources of Yorkshire*. Maney and Son, Leeds, 161–223.

Hermoso, M., Minoletti, F. *et al.* 2009. Global and local forcing of Early Toarcian seawater chemistry: a comparative study of different paleoceanographic settings (Paris and Lusitanian basins). *Paleoceanography*, **24**, https://doi.org/10.1029/2009pa001764

Hermoso, M., Minoletti, F., Rickaby, R.E.M., Hesselbo, S.P., Baudin, F. and Jenkyns, H.C. 2012. Dynamics of a stepped carbon-isotope excursion: ultra high-resolution study of Early Toarcian environmental change. *Earth and Planetary Science Letters*, **319–320**, 45–54, https://doi.org/10.1016/j.epsl.2011.12.021

Hesselbo, S.P. and King, C. 2019. Stratigraphic framework for the Yorkshire Lias. *In:* Lord, A.R. (ed.) *Fossils from the Lias of the Yorkshire Coast*. *Palaeontological Association Field Guide to Fossils*, 30–40.

Hesselbo, S.P. and Pieńkowski, G. 2011. Stepwise atmospheric carbon-isotope excursion during the Toarcian Oceanic Anoxic Event (Early Jurassic, Polish Basin). *Earth and Planetary Science Letters*, **301**, 365–372, https://doi.org/10.1016/j.epsl.2010.11.021

Hesselbo, S.P., Gröcke, D.R., Jenkyns, H.C., Bjerrum, C.J., Farrimond, P., Morgans Bell, H.S. and Green, O.R. 2000. Massive dissociation of gas hydrate during a Jurassic oceanic anoxic event. *Nature*, **406**, 392–395, https://doi.org/10.1038/35019044

Hesselbo, S.P., Jenkyns, H.C., Duarte, L.V. and Oliveira, L.C.V. 2007. Carbon-isotope record of the Early Jurassic (Toarcian) Oceanic Anoxic Event from fossil wood and marine carbonate (Lusitanian Basin, Portugal). *Earth and Planetary Science Letters*, **253**, 455–470, https://doi.org/10.1016/j.epsl.2006.11.009

Houben, A.J.P., Goldberg, T. and Slomp, C.P. 2021. Biogeochemical evolution and organic carbon deposition on the Northwestern European Shelf during the Toarcian Ocean Anoxic Event. *Palaeogeography, Palaeoclimatology, Palaeoecology*, **565**, 110191, https://doi.org/10.1016/j.palaeo.2020.110191

Howard, A.S. 1985. Lithostratigraphy of the Staithes Sandstone and Cleveland Ironstone formations (Lower Jurassic) of north-east Yorkshire. *Proceedings of the Yorkshire Geological Society*, **45**, 261–275, https://doi.org/10.1144/pygs.45.4.261

Howarth, M.K. 1955. Domerian of the Yorkshire Coast. *Proceedings of the Yorkshire Geological Society*, **30**, 147–175, https://doi.org/10.1144/pygs.30.2.147

Howarth, M.K. 1962. The Jet rock series and the alum shale series of the Yorkshire Coast. *Proceedings of the Yorkshire Geological Society*, **33**, 381–422, https://doi.org/10.1144/pygs.33.4.381

Howarth, M.K. 1973. The stratigraphy and ammonite fauna of the upper Liassic Grey Shales of the Yorkshire coast. *Bulletin of the British Museum (Natural History) Geology*, **24**, 235–277, https://doi.org/10.5962/p.313825

Howarth, M.K. 1992. The ammonite family hildoceratidae in the Lower Jurassic of Britain. *In*: *Monograph of the Palaeontographical Society*. The Palaeontographical Society, London, 106pp.

Ivimey-Cook, H.C. and Powell, J.H. 1991. Late Triassic and early Jurassic biostratigraphy of the Felixkirk Borehole, North Yorkshire. *Proceedings of the Yorkshire Geological Society*, **48**, 367–374, https://doi.org/10.1144/pygs.48.4.367

Jarvis, I. 2003. Sample preparation in ICP-MS. *In:*Jarvis, K.E., Gray, A.L. and Houk, R.S. (eds) *Handbook of Inductively Coupled Plasma Mass Spectrometry*. Viridian, Woking, 172–224.

Jenkyns, H.C. and Clayton, C.J. 1997. Lower Jurassic epicontinental carbonates and mudstones from England and Wales: chemostratigraphic signals and the early Toarcian anoxic event. *Sedimentology*, **44**, 687–706, https://doi.org/10.1046/j.1365-3091.1997.d01-43.x

Jenkyns, H.C. and Macfarlane, S. 2022. The chemostratigraphy and environmental significance of the Marlstone and Junction Bed (Beacon Limestone, Toarcian, Lower Jurassic, Dorset, UK). *Geological Magazine*, **159**, 357–371, https://doi.org/10.1017/S0016756821000972

Jenkyns, H.C., Gröcke, D.R. and Hesselbo, S.P. 2001. Nitrogen isotope evidence for water mass denitrification during the Early Toarcian (Jurassic) oceanic anoxic event. *Paleoceanography*, **16**, 593–603, https://doi.org/10.1029/2000PA000558

Kemp, D.B., Coe, A.L., Cohen, A.S. and Schwark, L. 2005. Astronomical pacing of methane release in the Early Jurassic period. *Nature*, **437**, 396–399, https://doi.org/10.1038/nature04037

Kemp, D.B., Coe, A.L., Cohen, A.S. and Weedon, G.P. 2011. Astronomical forcing and chronology of the early Toarcian (Early Jurassic) oceanic anoxic event in Yorkshire, UK. *Paleoceanography*, **26**, https://doi.org/10.1029/2011PA002122

Kent, P.E. 1980. Subsidence and uplift in East Yorkshire and Lincolnshire: a double inversion. *Proceedings of the Yorkshire Geological Society*, **42**, 505–524, https://doi.org/10.1144/pygs.42.4.505

Krencker, F.-N., Bodin, S., Suan, G., Heimhofer, U., Kabiri, L. and Immenhauser, A. 2015. Toarcian extreme warmth led to tropical cyclone intensification. *Earth and Planetary Science Letters*, **425**, 120–130, https://doi.org/10.1016/j.epsl.2015.06.003

Lazar, O.R., Bohacs, K.M., Macquaker, J.H.S., Schieber, J. and Demko, T.M. 2015. Capturing key attributes of fine-grained sedimentary rocks in outcrops, cores, and thin sections: nomenclature and description guidelines. *Journal of Sedimentary Research*, **85**, 230–246, https://doi.org/10.2110/jsr.2015.11

Littler, K., Hesselbo, S.P. and Jenkyns, H.C. 2010. A carbon-isotope perturbation at the Pliensbachian–Toarcian boundary: evidence from the Lias Group, NE England. *Geological Magazine*, **147**, 181–192, https://doi.org/10.1017/S0016756809990458

Marsaglia, K.M. and Klein, G.D. 1983. The paleogeography of Paleozoic and Mesozoic storm depositional systems. *The Journal of Geology*, **91**, 117–142, https://doi.org/10.1086/628752

März, C., Wagner, T. *et al.* 2016. Repeated enrichment of trace metals and organic carbon on an Eocene high-energy shelf caused by anoxia and reworking. *Geology*, **44**, 1011–1014, https://doi.org/10.1130/G38412.1

McArthur, J.M., Algeo, T.J., Schootbrugge, B.van de, Li, Q. and Howarth, R.J. 2008. Basinal restriction, black shales, Re-Os dating, and the Early Toarcian (Jurassic) oceanic anoxic event. *Paleoceanography*, **23**, https://doi.org/10.1029/2008PA001607

McArthur, J.M. 2019. Early Toarcian black shales: A response to an oceanic anoxic event or anoxia in marginal basins? *Chemical Geology*, **522**, 71–83, https://doi.org/10.1016/j.chemgeo.2019.05.028

McCave, I.N., Manighetti, B. and Robinson, S.G. 1995. Sortable silt and fine sediment size/composition slicing: parameters for palaeocurrent speed and palaeoceanography. *Paleoceanography*, **10**, 593–610, https://doi.org/10.1029/94PA03039

McKee, E.D. and Weir, G.W. 1953. Terminology for stratification and cross-stratification in sedimentary rocks. *GSA Bulletin*, **64**, 381–390, https://doi.org/10.1130/0016-7606(1953)64[381:TFSACI]2.0.CO;2

O'Brien, N.R. 1990. Significance of lamination in Toarcian (Lower Jurassic) shales from Yorkshire, Great Britain. *Sedimentary Geology*, **67**, 25–34, https://doi.org/10.1016/0037-0738(90)90025-O

Pittet, B., Suan, G., Lenoir, F., Duarte, L.V. and Mattioli, E. 2014. Carbon isotope evidence for sedimentary discontinuities in the lower Toarcian of the Lusitanian Basin (Portugal): sea level change at the onset of the Oceanic Anoxic Event. *Sedimentary Geology*, **303**, 1–14, https://doi.org/10.1016/j.sedgeo.2014.01.001

Powell, J.H. 1984. Lithostratigraphical nomenclature of the Lias Group in the Yorkshire Basin. *Proceedings of the Yorkshire Geological and Polytechnic Society*, **45**, 51–57, https://doi.org/10.1144/pygs.45.1-2.51

Powell, J.H. 2010. Jurassic sedimentation in the Cleveland Basin: a review. *Proceedings of the Yorkshire Geological Society*, **58**, 21–72, https://doi.org/10.1144/pygs.58.1.278

Pye, K. and Krinsley, D.H. 1986. Microfabric, mineralogy and early diagenetic history of the Whitby Mudstone Formation (Toarcian), Cleveland Basin, U.K. *Geological Magazine*, **123**, 191–203, https://doi.org/10.1017/S0016756800034695

Rawson, P.F. and Wright, J.K. 1995. Jurassic of the Cleveland Basin, North Yorkshire. *In:* Taylor, P.D. (ed.) *Field Geology of the British Jurassic*. The Geological Society, London, 173–208.

Remírez, M.N. and Algeo, T.J. 2020. Paleosalinity determination in ancient epicontinental seas: a case study of the T-OAE in the Cleveland Basin (UK). *Earth-Science Reviews*, **201**, 103072, https://doi.org/10.1016/j.earscirev.2019.103072

Storm, M.S., Hesselbo, S.P. *et al.* 2020. Orbital pacing and secular evolution of the Early Jurassic carbon cycle. *Proceedings of the National Academy of Sciences*, **117**, 3974–3982, https://doi.org/10.1073/pnas.1912094117

Studholme, J., Fedorov, A.V., Gulev, S.K., Emanuel, K. and Hodges, K. 2022. Poleward expansion of tropical cyclone latitudes in warming climates. *Nature Geoscience*, **15**, 14–28, https://doi.org/10.1038/s41561-021-00859-1

Them, T.R., Gill, B.C. *et al.* 2017. High-resolution carbon isotope records of the Toarcian Oceanic Anoxic Event (Early Jurassic) from North America and implications for the global drivers of the Toarcian carbon cycle. *Earth and Planetary Science Letters*, **459**, 118–126, https://doi.org/10.1016/j.epsl.2016.11.021

Them, T.R., Gill, B.C. *et al.* 2018. Thallium isotopes reveal protracted anoxia during the Toarcian (Early Jurassic) associated with volcanism, carbon burial, and mass extinction. *Proceedings of the National Academy of Sciences*, **115**, 6596–6601, https://doi.org/10.1073/pnas.1803478115

Thibault, N., Ruhl, M., Ullmann, C.V., Korte, C., Kemp, D.B., Gröcke, D.R. and Hesselbo, S.P. 2018. The wider context of the Lower Jurassic Toarcian oceanic anoxic event in Yorkshire coastal outcrops, UK. *Proceedings of the Geologists' Association*, **129**, 372–391, https://doi.org/10.1016/j.pgeola.2017.10.007

Trabucho-Alexandre, J. 2015. More gaps than shale: erosion of mud and its effect on preserved geochemical and palaeobiological signals. *Geological Society, London, Special Publications*, **404**, 251–270, https://doi.org/10.1144/SP404.10

Trabucho-Alexandre, J., Dirkx, R., Veld, H., Klaver, G. and Boer, P.L.de 2012. Toarcian black shales in the Dutch Central Graben: Record of energetic, variable depositional conditions during an oceanic anoxic event. *Journal of Sedimentary Research*, **82**, 104–120, https://doi.org/10.2110/jsr.2012.5

Tribovillard, N., Koched, H., Baudin, F., Adatte, T., Delattre, M., Abraham, R. and Ferry, J.-N. 2019. Storm-induced concentration of sulfurized, marine-origin, organic matter as a possible mechanism in the formation of petroleum source-rock. *Marine and Petroleum Geology*, **109**, 808–818, https://doi.org/10.1016/j.marpetgeo.2019.07.003

Van de Schootbrugge, B., Houben, A.J.P. *et al.* 2020. Enhanced Arctic-Tethys connectivity ended the Toarcian Oceanic Anoxic Event in NW Europe. *Geological Magazine*, **157**, 1593–1611, https://doi.org/10.1017/S0016756819001262

Warme, J.E. 1991. Delmar Formation and Torrey Sandstone as exposed along beach cliffs, Solana Beach, northern San Diego County. *In:*Abbott, P.L. and May, J.A. (eds) *Eocene Geologic History San Diego Region*. The Pacific Section of the Society of Economic Paleontologists and Mineralogists, Los Angeles, CA, 39–54.

Wignall, P.B., Newton, R.J. and Little, C.T.S. 2005. The timing of paleoenvironmental change and cause-and-effect relationships during the early Jurassic mass extinction in Europe. *American Journal of Science*, **305**, 1014–1032, https://doi.org/10.2475/ajs.305.10.1014

Wong, T.E. 2007. Jurassic. *In:* Wong, T.E., Batjes, D.A.J. and de Jager, J. (eds) *Geology of the Netherlands*. Royal Netherlands Academy of Arts and Sciences, Amsterdam, 107–125.

Wright, J.K. 2022. The Market Weighton High in the 21st century – new understanding of a long-standing problem. *Proceedings of the Yorkshire Geological Society*, **64**, https://doi.org/10.1144/pygs2021-008

Xu, W., Ruhl, M. *et al.* 2018. Evolution of the Toarcian (Early Jurassic) carbon-cycle and global climatic controls on local sedimentary processes (Cardigan Bay Basin, UK). *Earth and Planetary Science Letters*, **484**, 396–411, https://doi.org/10.1016/j.epsl.2017.12.037

Yawar, Z. and Schieber, J. 2017. On the origin of silt laminae in laminated shales. *Sedimentary Geology*, **360**, 22–34, https://doi.org/10.1016/j.sedgeo.2017.09.001

Ziegler, P.A. 1981. Evolution of sedimentary basins of North-West Europe. *In:* Illing, L.V. and Hobson, G.D. (eds) *Petroleum Geology of the Continental Shelf of North-West Europe*. Institute of Petroleum, London, 3–39.

Ziegler, P.A. 1990. *Geological Atlas of Western and Central Europe*. 2nd edn. Shell Internationale Petroleum Maatschappij, The Hague.